Evolution of a Coupled Marine Ice Sheet–Sea Level Model

Evolution of a coupled marine ice sheet–sea level model

Natalya Gomez,[1] David Pollard,[2] Jerry X. Mitrovica,[1] Peter Huybers,[1] and Peter U. Clark[3]

Received 16 June 2011; revised 18 November 2011; accepted 6 December 2011; published 14 February 2012.

[1] We investigate the stability of marine ice sheets by coupling a gravitationally self-consistent sea level model valid for a self-gravitating, viscoelastically deforming Earth to a 1-D marine ice sheet-shelf model. The evolution of the coupled model is explored for a suite of simulations in which we vary the bed slope and the forcing that initiates retreat. We find that the sea level fall at the grounding line associated with a retreating ice sheet acts to slow the retreat; in simulations with shallow reversed bed slopes and/or small external forcing, the drop in sea level can be sufficient to halt the retreat. The rate of sea level change at the grounding line has an elastic component due to ongoing changes in ice sheet geometry, and a viscous component due to past ice and ocean load changes. When the ice sheet model is forced from steady state, on short timescales (<∼500 years), viscous effects may be ignored and grounding-line migration at a given time will depend on the local bedrock topography and on contemporaneous sea level changes driven by ongoing ice sheet mass flux. On longer timescales, an accurate assessment of the present stability of a marine ice sheet requires knowledge of its past evolution.

Citation: Gomez, N., D. Pollard, J. X. Mitrovica, P. Huybers, and P. U. Clark (2012), Evolution of a coupled marine ice sheet–sea level model, *J. Geophys. Res.*, *117*, F01013, doi:10.1029/2011JF002128.

1. Introduction

[2] The stability of polar ice sheets, and in particular that of the West Antarctic Ice Sheet (WAIS), is of central concern within studies of modern climate change [*Lenton et al.*, 2008; *Smith et al.*, 2009]. The WAIS is a marine-based ice sheet that interacts with the surrounding ocean. The ice shelves that fringe the WAIS are known to have a stabilizing or buttressing effect on the ice sheet [*Thomas and Bentley*, 1978; *Dupont and Alley*, 2005; *Goldberg et al.*, 2009], but these shelves appear susceptible to climate change since warming of the atmosphere and/or ocean could lead to increased melting and disintegration either from above and/or below, respectively [*Jenkins and Doake*, 1991; *Rignot and Jacobs*, 2002; *MacAyeal et al.*, 2003]. Indeed, collapse of ice shelves as well as thinning, retreat and acceleration of outlet glaciers have recently been observed in various sectors of the WAIS [e.g., *Shepherd et al.*, 2001; *Thomas et al.*, 2004; *Rignot*, 2006; *Wingham et al.*, 2009].

[3] Marine ice sheets gain mass by accumulation throughout their interior and they lose mass by flux of ice across the grounding line into floating ice shelves. The grounding-line zone is located where the ice changes from being thick enough to keep the base of the ice grounded on bedrock below the local sea surface, to thin enough that the ice floats, dividing the floating ice shelves from the grounded ice sheet. Ice thickness at the grounding line is approximately proportional to the depth of water; in order for the ice sheet to come into equilibrium after an increase in water depth requires the grounding line to shift toward a shallower location [*Weertman*, 1974; *Thomas and Bentley*, 1978; *Schoof*, 2007]. *Weertman* [1974] used a steady state ice sheet model to argue that marine ice sheets resting on reversed bed slopes (i.e., sloping down toward the interior) are unstable and prone to rapid retreat [see also *Thomas and Bentley*, 1978]. This so-called Marine Ice Sheet Instability Hypothesis is based on the premise (supported by analysis in the references above) that ice velocity across the grounding line depends very strongly on grounding-line depth, so as the grounding line retreats into deeper water, the rapidly increasing flux of ice across the grounding line causes drawdown of upstream grounded ice and an accelerating grounding-line retreat. These conclusions have been confirmed in recent studies that have extended these canonical analyses to include ice-shelf buttressing, boundary layers to model the ice sheet/ice-shelf transition zone and an extension to three spatial dimensions [e.g., *Dupont and Alley*, 2005; *Schoof*, 2007; *Goldberg et al.*, 2009; *Katz and Worster*, 2010].

[4] In general, investigations of marine ice sheet stability have either ignored sea level changes associated with ice-mass changes, or included them by assuming that such changes are geographically uniform [*Thomas and Bentley*, 1978; *Schoof*, 2007; *Wilchinsky*, 2009]. However, gravitationally self-consistent predictions of sea level change following the retreat or advance of grounded ice sheets or glaciers are characterized by dramatically non-uniform

[1]Department of Earth and Planetary Sciences, Harvard University, Cambridge, Massachusetts, USA.
[2]Earth and Environmental Systems Institute, Pennsylvania State University, University Park, Pennsylvania, USA.
[3]Department of Geosciences, Oregon State University, Corvallis, Oregon, USA.

0148-0227/12/2011JF002128

geometries. In particular, in the vicinity of a rapidly melting ice sheet (i.e., within ~2000 km), sea level will fall as a consequence of instantaneous gravitational and deformational effects [*Farrell and Clark*, 1976; *Mitrovica et al.*, 2001; *Gomez et al.*, 2010a]. These effects also contribute to a geographically variable pattern of sea level rise predicted for sites at greater distances from the ice sheet. *Gomez et al.* [2010b] coupled predictions of this instantaneous sea level fingerprint to the *Weertman* [1974] steady state 1-D ice sheet model, and they demonstrated that on a reversed bed, the sea level fall resulting from ice loss compensates for the deepening of the bed, and for some reversed bed slopes this compensation is sufficient to stabilize the ice sheet.

[5] The present analysis extends the work of *Gomez et al.* [2010b] by rigorously introducing the dimension of time, i.e., we move beyond simple descriptions of instability versus stability to assess the timescale of retreat for a range of ice sheet forcings. This analysis requires more complex sea level and ice sheet models. The sea level fingerprints used by *Gomez et al.* [2010b] are valid for melting events with a timescale less than the Maxwell time over which the solid Earth deforms elastically (~500 years). However, large-scale changes in ice sheets can take place over several thousand years or longer, and on these timescales, the viscous response of the upper mantle and crust, which will be a function of the entire pre-history of ice and ocean loading, can contribute significantly to local changes in sea level. In this case, the elastic and viscous responses combine to produce, for example, a localized zone of crustal uplift in the vicinity of a melting ice sheet and a subsidence of surrounding forebulges as the system relaxes toward isostatic equilibrium. To model such effects, we adopt a gravitationally self-consistent sea level model that accounts for the deformation of a self-gravitating, viscoelastic Earth model [*Kendall et al.*, 2005; *Gomez et al.*, 2010a]. In addition, *Weertman*'s [1974] ice sheet model considered only the stability of steady state ice sheet configurations. Here we employ a dynamic ice sheet model [*Pollard and DeConto*, 2007, 2009] to investigate how sea level changes influence the timescale and extent of retreat of a marine ice sheet subject to a perturbation in climate.

2. Model Setup

2.1. Ice Sheet Model

[6] We adopt a 1-D, axisymmetric version of the ice sheet-shelf model described by *Pollard and DeConto* [2007, 2009]. In this type of model, long-term variations of ice thickness are stepped forward in time, accounting for net horizontal advection by ice flow, annual accumulation minus ablation on the ice surface, and any melting or freeze-on at the base. Our model heuristically combines the scaled equations for grounded (shearing) flow and for floating or stream (stretching) flow. The grounding-line zone acts as a boundary layer between the two flow regimes, and a recent parameterization of ice velocity at the grounding line [*Schoof*, 2007] captures the effect of the grounding-line zone on the large-scale flow in the model and avoids the need for very fine resolution to resolve explicitly variations through the grounding-zone boundary layer. Following *Schoof* [2007], this parameterization also incorporates buttressing of the upstream flow by ice shelves. In addition, the model predicts ice thickness variations due to mass advection and surface mass balance. For all runs here, ice temperatures and thermal effects are not included, and ice rheology is uniform with a Glen flow law exponent of 3 and a coefficient of 2×10^{-16} Pa^{-3} a^{-1}. Basal sliding occurs wherever the ice is grounded. The sliding velocity is given by $u_b = B\,\tau_b^2$, where τ_b is basal shear stress and $B = 10^{-10}$ m a^{-1} Pa^{-2} is the sliding coefficient. Unless otherwise specified, surface accumulation everywhere is 0.1 m a^{-1} ice equivalent with no seasonal or interannual variability, and there is no sub-ice shelf oceanic melting. At the most peripheral grid point (right-hand side of the plots below), ice thickness is set to zero, which is equivalent to allowing free flow of ice out of the model domain and has no upstream effect. The interior edge of the domain (left-hand side of the plots below) is a divide, i.e., where the ice elevation is maximum, and surface slope and ice flux are zero; this is nominally the South Pole for the idealized model here, but would be the limit of the catchment area for real glacier systems. The ice sheet domain is regularly gridded in latitude at 0.1° latitude (~11 km) and irregularly gridded in the vertical into ten intervals, and the model time step is 0.1 yr. Note that the results of experiments with twice the spatial resolution and shorter time steps showed no significant differences from the results presented here.

[7] Floating ice shelves affect upstream flow and grounding-line migration by their back stress ("buttressing") at the grounding line [e.g., *Schoof*, 2007]. Back stress is caused by the ice shelf moving past or abutting land or grounded ice (called "side drag" here), or by bedrock pinning points impinging on its base. In their absence, a freely floating ice shelf would provide zero back stress at the grounding line, and would have no dynamical effect on grounding-line position or on upstream grounded flow if it were to break up entirely; conversely, breakup of a previously buttressing ice shelf can cause dramatic upstream acceleration, drawdown of grounded ice, and grounding-line retreat [*Scambos et al.*, 2004; *Schoof*, 2007]. To include buttressing effects in idealized 1-D flow line studies, side drag or pinning points must be parameterized [*Dupont and Alley*, 2005; *Goldberg et al.*, 2009; *Gagliardini et al.*, 2010]. Here, a retarding stress per unit horizontal area is applied in the momentum equation where ice is floating, proportional to ice thickness and velocity, and independent of flow band width (similar to *Gagliardini et al.* [2010]),

$$SD = -K\,u_a\,h, \tag{1}$$

where SD is the retarding stress (N m^{-2}), K is a coefficient with nominal value 3×10^{-4} N a m^{-4}, u_a is ice-shelf horizontal velocity (m a^{-1}), and h is ice-shelf thickness (m). This simple parameterization can be considered to represent either side drag or pinning points equally well; in reality, both probably depend on ice thickness and velocity with at least the same sign as in equation (1) (but note that we use the phrase "side drag" for brevity throughout this paper). The nominal magnitude of K is selected to produce reasonable pre-perturbation states in the flow line model; more direct connection with reality will require 3-D modeling with explicit side-shear geometry and pinning-point bathymetry.

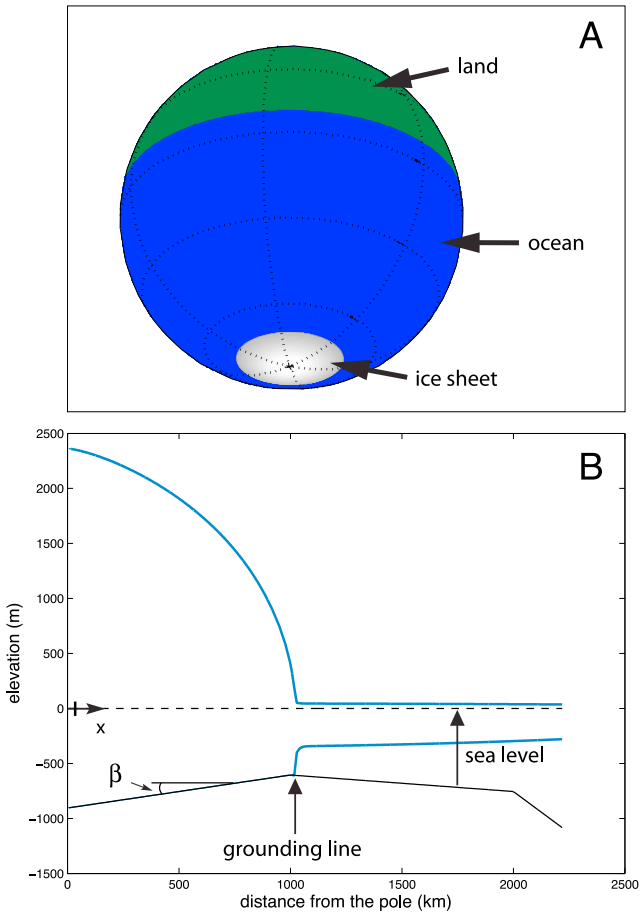

Figure 1. Schematic illustrating the initial steady state model configuration. (a) The axisymmetric configuration of the model Earth, which includes an ocean covering 70% of the surface area of the Earth (blue), a spherical cap continent at the North Pole (green), and a circular disk ice sheet on the South Pole (white). (b) Cross section of the ice sheet in Figure 1a. The blue lines represent the elevation of the surface of the ice and the bottom of the ice shelf. The solid black line represents the elevation of the bedrock and the dashed black line at zero elevation represents the sea surface. The ice sheet's grounding line, corresponding to the junction of the solid blue and black lines, is initially located just outside of a region where the bed slopes down to the center of the ice sheet with slope β.

2.2. Sea Level Model

[8] In a static (or equilibrium) sea level theory, the sea surface is defined to lie on a gravitational equipotential surface, and sea level is the difference between the radial positions (i.e., directed along a line out from the center of the unperturbed Earth) of this gravitational equipotential and the solid surface [*Farrell and Clark*, 1976; *Dahlen*, 1976]. Following this definition, sea level is defined globally, i.e., over oceans and continents, and it is equivalent to the negative of topography, where topography is defined to exclude ice height and is thus synonymous with bedrock elevation.

[9] We adopt the generalized, gravitationally self-consistent sea level theory described in detail by *Kendall et al.* [2005] and *Gomez et al.* [2010a]. In particular, we use the version of this theory valid for a spherically symmetric, self-gravitating, Maxwell viscoelastic Earth model (here called the GSCVE sea level theory). The depth-dependent variations in the elastic and density structure in the Earth model are given by the seismic model PREM [*Dziewonski and Anderson*, 1981]. The viscosity structure is discretized into three layers: an infinite viscosity (i.e., elastic) lithosphere of thickness 120 km, an upper mantle viscosity of 5×10^{20} Pa s and a lower mantle viscosity of 5×10^{21} Pa s. This viscosity profile is consistent with most inferences based on ice-age data sets [*Lambeck et al.*, 1998; *Mitrovica and Forte*, 2004]. The GSCVE sea level model accounts for the exchange of mass between grounded ice and ocean and incorporates time-dependent shoreline migration, allowing for the inundation of water into areas freed of marine-based ice. Since the model is gravitationally self-consistent, deformation of the solid surface and the sea surface equipotential are coupled, i.e., deformation of the solid Earth alters the gravitational field and thus perturbs the sea surface. The latter impacts the distribution of water in the model, and this redistribution will, in turn, deform the solid Earth.

[10] Figure 1a shows the axisymmetric continent configuration adopted in our model. It is comprised of two regions: a continent with bedrock below the sea surface at the South Pole on which the ice sheet sits (see discussion of Figure 1b below) and a spherical cap continent centered at the North Pole with elevation above the sea surface elevation. The area of the latter is chosen such that 70% of the surface area of the Earth is covered by ocean and ice shelves in the initial configuration of the Antarctic Ice Sheet model. The initial state of the ice, bedrock and ocean is assumed to be in isostatic equilibrium, and the sea level model predicts changes from this state as the ice sheet evolves, as described in section 2.3. Sea level calculations are performed with a truncation at spherical harmonic degree 512 (i.e., a spatial resolution of ~40 km).

2.3. Ice Sheet: Sea Level Coupling

[11] We perform a two-way coupling between the ice sheet and sea level models described above. Predictions of current sea level in the model are used to update bedrock topography in the ice sheet model. Conversely, predictions of ice geometry in the ice sheet model are used to specify ice loading in the sea level model. In the simulations described below, the ice sheet model is run continuously for 10,000 years. Every 50 years, the current ice geometry is passed to the sea level model, which computes the sea level change (or equivalently, the negative of the bedrock elevation change) over the last 50-year interval. The current sea level field is updated accordingly and passed back to the ice sheet model. Passed fields are linearly interpolated in latitude between the two model grids. Note that we also ran a series of simulations with shorter coupling time intervals and these results showed no significant differences from the simulations shown here using a 50 year interval.

[12] As discussed above, the change in the current sea level computed by the GSCVE sea level model is a combination of (1) an instantaneous elastic deformation of the solid Earth and perturbation to the sea surface equipotential driven by contemporaneous ice and ocean load changes and

(2) a delayed viscous response of the solid Earth (and associated gravitational effects) that depends on the entire history of ice and ocean loading. In order to model the viscous response, the GSCVE sea level model stores the entire sequence of 50-year-interval ice geometries from the start of the run, and uses them to compute the current sea level each time it is called. A critical quantity that we must track for the purpose of coupling the sea level and ice sheet models is the distance between the surface that the ice rests upon and the gravitational equipotential that defines the sea surface. This distance governs the buoyancy of grounded ice. We specify the equipotential sea surface as zero elevation in the ice sheet model, and in this reference frame changes in bedrock elevation are equivalent to the negative of changes in sea level. This relationship permits a simple coupling of the two models.

[13] As noted above, the ice sheet model domain is axisymmetric in longitude, with only one grid cell in the east–west direction. Within the ice sheet model, the longitudinal arc-width of the flow band is arbitrary. The arc-width is specified as 360° for coupling to the sea level model, which is global in extent and axisymmetric, i.e., as shown in Figure 1a, and which involves an ice sheet that is modeled as a circular disk centered on the South Pole. As discussed below, future work will address more realistic geometries associated with specific Antarctic sectors.

3. Experiments

[14] In this section, we consider the impact of the sea level coupling on the ice sheet response to a prescribed external forcing for a range of parameter choices and timescales. The ice sheet model is initially run to the steady state configuration illustrated in Figure 1b. The ice sheet's grounding line is initially located 10 km outside a region where the bed inclines down to the center of the ice sheet with slope β.

[15] In many of the experiments below, the external forcing is a reduction in ice-shelf buttressing, imposed by reducing the side-drag coefficient K in equation (1). The model would also respond similarly if, for instance, sub-ice-shelf oceanic melt rates (zero in all experiments here) were increased, which would thin the ice shelf and reduce side drag through the term h in equation (1). However, in line with the idealized geometry and to simplify the interpretation of results, we have chosen to reduce K directly. Actual reductions of buttressing in real Antarctic ice shelves stemming from atmospheric and oceanic forcing are deferred to future 3-D modeling.

[16] In the first set of experiments (Figure 2), the side-drag coefficient K is instantaneously reduced at time t = 0 from its nominal value, which increases the flux of ice across the grounding line, causing the grounding line to retreat onto the reversed bed slope. As an example, Figure 2a shows the evolution of the ice sheet along a reversed bed slope of $\beta = -0.7$ m/km following a reduction in K to 2/3 its nominal value. In this example, the positions of the bedrock and sea-surface equipotential stay constant (i.e., the sea level coupling is not included). Once the grounding line reaches the reversed slope, a small additional retreat moves the grounding line into deeper water, leading to a greater ice loss across the grounding line and further retreat. As a consequence, the ice sheet retreats down the slope until it disappears. The full retreat takes approximately 4000 model years.

[17] Next, we explore the implications for this particular scenario of adding the sea level coupling to the ice sheet model (Figure 2b). In this case, as the ice sheet retreats, sea level falls, or equivalently, the bedrock elevation relative to the sea-surface height increases (the black line in Figure 2b deforms upwards). Thus, the water level is shallower at the new grounding line than predicted in the simulation where sea level remained fixed (Figure 2a). The rate of ice loss across the grounding line is slower than in the fixed-bed case and the retreat is slowed. The ice sheet takes ~7300 years to disappear, or 1.8 times longer than predicted in Figure 2a.

[18] Figure 2c shows the sea level change relative to the initial steady state (i.e., relative to the horizontal line) at each time step of the ice sheet evolution plotted in Figure 2b. As described above, the sea level changes are applied as a perturbation to the bedrock topography in Figure 2b. Elastic effects dominate the sea level change 1000 years into the evolution. As the ice sheet loses mass over this time interval, the gravitational attraction it exerts on the surrounding water weakens and, in response, water migrates away. In addition, the solid Earth in the vicinity of the ice loss and water outflux rebounds elastically. Both of these effects contribute to the sea level fall predicted by the GSCVE sea level model at the grounding line [*Gomez et al.*, 2010b]. In subsequent time steps, the viscous effects also act to raise the bedrock at the grounding line, thus elastic and viscous effects combine to produce a further decrease in sea level. Note that since gravitational and deformation effects are coupled (see Section 2.2), raising the solid surface toward isostatic equilibrium counters the direct gravitational effect of ice loss (i.e., the net negative mass anomaly created by past ice loss and solid Earth deformation tends to zero as the solid surface rebounds toward isostatic equilibrium). However, this signal is swamped by deformation driven by the ongoing ice mass loss. Within a given time interval, the fall in sea level is greatest in the region across which the grounding line migrates (i.e., the maximum drop in the sea level curves in Figure 2c are located near the corresponding grounding line location in Figure 2b).

[19] When the external forcing imposed through a reduction in the side–drag coefficient and/or the reversed bed slope are sufficiently small, the fall in sea level that accompanies ice sheet retreat will be large enough that the ice sheet stabilizes to a new steady state. An illustrative scenario is shown in Figures 2d–2f for the case of an ice sheet resting on a bed slope that is initially −0.3 m/km, which is less steep than the value adopted in Figures 2a–2c (−0.7 m/km). In Figure 2d, the bedrock and sea-surface elevations are held constant and the ice sheet disappears in ~7200 years. In contrast, when the sea level coupling is included in Figure 2e, the sea level fall (Figure 2f) is sufficient to halt the ice sheet retreat. The ice sheet reaches a new equilibrium with the grounding line located ~200 km inland of its initial position. Note in Figure 2f that as the ice sheet reaches a new equilibrium, ongoing viscous deformation toward isostatic equilibrium causes sea level to continue to fall. This residual sea level change further stabilizes the ice

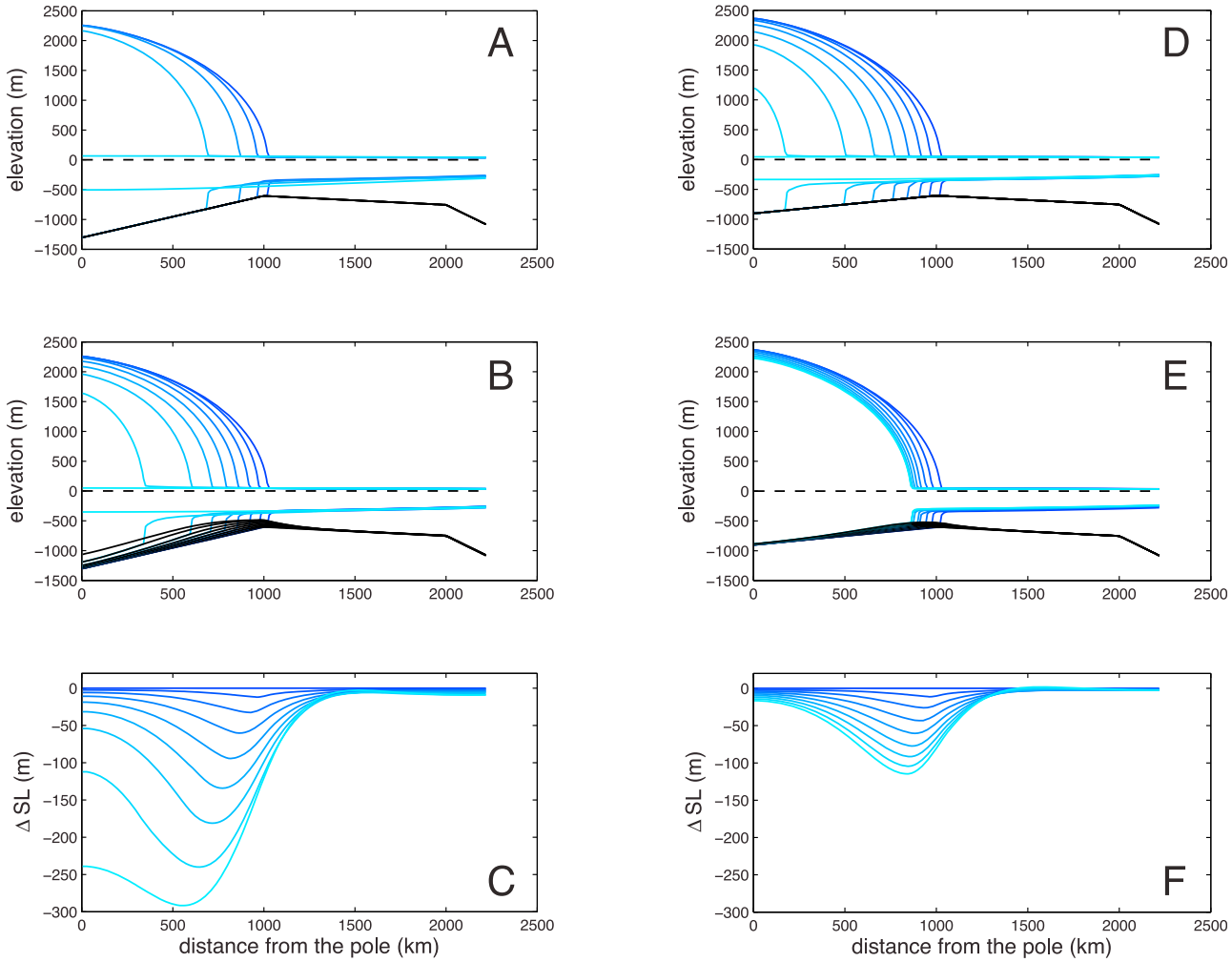

Figure 2. The evolution of the ice sheet shown in Figure 1b following a reduction in the side-drag coefficient to 2/3 its nominal value. Ice and bedrock elevation contours are plotted every 1000 years, and the ice contours move from dark to light blue as time increases. (a and b) The retreat along a reversed bed of slope −0.7 m/km in the fixed topography (Figure 2a) and topography that is updated by the sea level model every 50 years (Figure 2b). (c) Sea level change in the scenario of Figure 2b relative to the initial steady state, plotted every 1000 years. (d–f) Analogous to Figures 2a–2c for retreat along a bed slope of −0.3 m/km.

sheet and may lead to a future re-advance. Animations of the scenarios in Figure 2 are provided in the auxiliary material.[1]

3.1. Bed Slope and Forcing Parameters

[20] In this section, we discuss results of sensitivity analyses that vary several key aspects of the ice sheet model. To begin, we investigate further the influence of changing the bed slope adopted in the initial steady state configuration of the model. In Figure 3a, we initiate ice sheet retreat with a fixed, 60% reduction in the side-drag coefficient, and track the location of the grounding line as a function of time for simulations with a range of initially reversed bed slopes. The green lines are results of simulations in which sea level is fixed (i.e., as in Figures 2a and 2d) while the blue lines plot the grounding-line position when sea level changes are coupled with the ice sheet model (as in Figures 2b and 2e). In all cases where sea level is fixed, the grounding line retreats down the reversed slope until the ice sheet completely disappears, and the time scale of collapse increases with progressively shallower slopes. Once again, the inclusion of the sea level coupling acts to slow the rate of retreat. For initial bed profiles that are horizontal or have a relatively shallow slope (β = −0.3 m/km), the sea level fall at the grounding line is ultimately sufficient to halt the retreat and the ice sheets reach a new steady state 200 km and 300 km inward, respectively, of the original grounding line.

[21] Next, we consider the effect of varying the strength of the forcing that is applied to initiate the retreat. Figure 3b plots the grounding-line position as a function of time for simulations on a reversed bed slope of 0.3 m/km and a range of reductions in the ice-shelf side-drag coefficient K in equation (1). In the case where sea level is fixed, the speed of grounding-line retreat increases with greater reductions in

[1]Auxiliary materials are available in the HTML. doi:10.1029/2011JF002128.

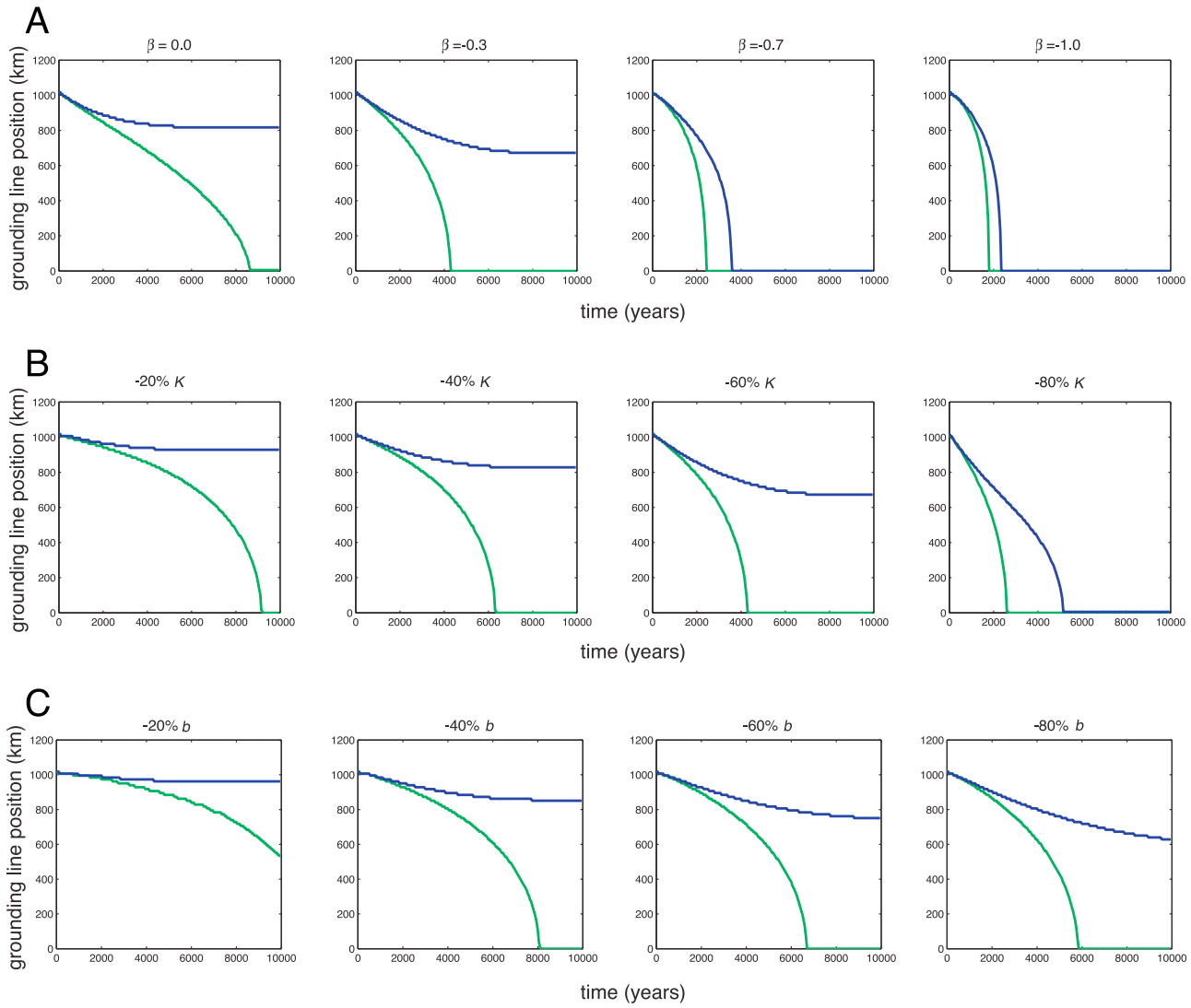

Figure 3. Grounding-line position as a function of time for (a) ice sheet retreat initiated by a fixed 60% reduction in the side-drag coefficient, K, down a range of reversed bed slopes of magnitude 0.0 to 1.0 m/km (as labeled). (b) As in Figure 3a except for reductions in the side-drag coefficient within the range 20%–80% of the nominal value and a fixed bed slope of −0.3 m/km. (c) As in Figure 3b, except that the side-drag coefficient is fixed and retreat is instead initiated by a reduction in the accumulation rate, b, of 20–80% of the nominal rate of 0.1 m a^{-1}. The green lines are results when sea level change is not coupled into the ice sheet model, whereas the blue lines include this coupling.

K, and thus the time scale for complete collapse decreases. The inclusion of the sea level coupling once again acts either to halt (Figure 3b, with a 20%, 40%, or 60% reduction in K) or slow down (by a factor of ∼2 with an 80% reduction in K) the retreat.

[22] In addition to driving retreat by reducing the side-drag coefficient, we also initiated ice sheet retreat by reducing the rate of accumulation. The results presented in Figure 3c show similar trends to those evident in Figure 3b except that the ice sheet responds less strongly to accumulation changes than to the same percentage change in the side-drag coefficient. In addition, in order to initiate retreat onto the reversed slope, these simulations prescribe rates of accumulation that are lower than the range expected over the Antarctic Ice Sheet. This difference in response is not surprising since marine ice in the Antarctic is generally more sensitive to changes in ocean temperature than to changes in accumulation rates and surface melting [*Jenkins and Doake*, 1991; *Rignot and Jacobs*, 2002; *MacAyeal et al.*, 2003]. Thus, reducing the ice-shelf buttressing effect (through a reduction in side drag) was found to be a more effective way of initiating retreat.

[23] Finally, in Figure 4 we summarize a large sequence of results based on simulations with a range of external forcing and bed slope combinations. In particular, Figure 4a plots the ratio of the time taken for the grounding line to retreat 200 km in simulations based on the coupled ice sheet-sea level model relative to simulations in which sea level is fixed in time. Figure 4b shows analogous results for a grounding line retreat of 500 km, i.e., the contours in Figure 4 represent

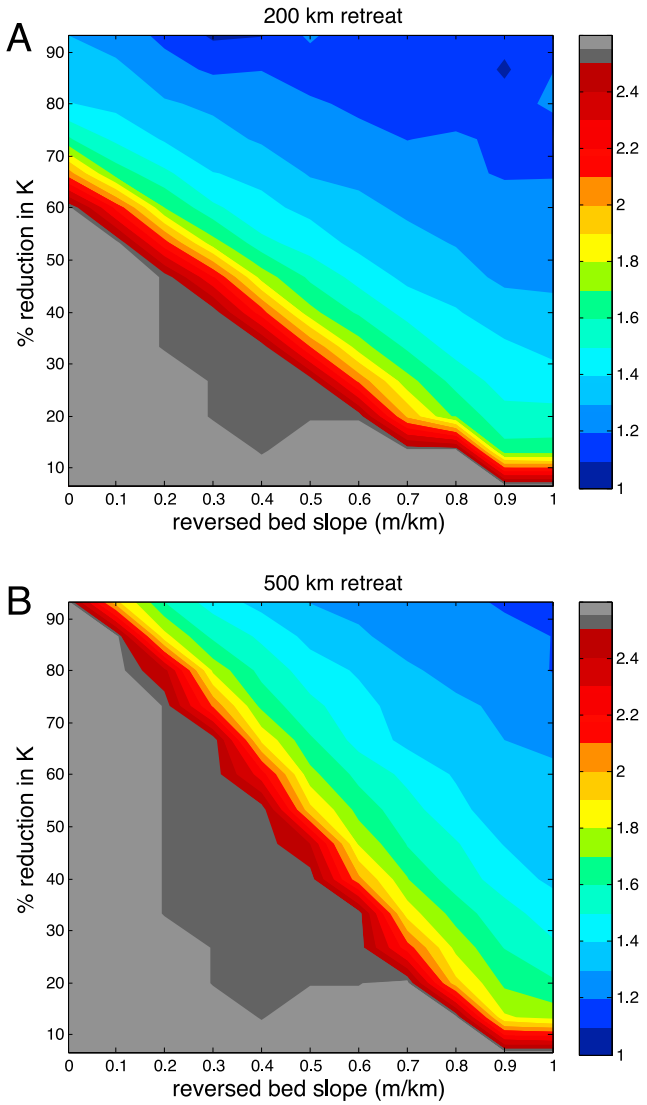

Figure 4. The ratio of the time scale of ice sheet retreat including sea level change coupling to the case without this coupling. Results are contoured as a function of bed slope and the percent reduction in side-drag coefficient K, where the latter is used to initiate retreat. The frames refer to time scales required for a retreat of either (a) 200 km or (b) 500 km and a total simulation time of 10,000 years. The gray contours represent simulations in which the coupled model does not retreat to the target distance within the 10,000 year simulation time, either because the retreat is too slow (dark gray) or the system reaches a new equilibrium (light gray).

the multiplicative factor by which the time scale of retreat is extended as a consequence of the inclusion of the GSCVE sea level model. In some simulations the grounding line does not retreat by the target distance within the 10,000 year model run either because a new steady state is reached (indicated by light gray contours) or because the retreat velocity is too small (dark gray contour). As an example, if the side-drag coefficient is reduced by half its nominal value on a reversed bed slope of −0.7 m/km, the inclusion of the sea level feedback in the ice sheet model extends the time scale by a factor of ∼1.3 for a 200 km retreat and by a factor of ∼1.6 for a 500 km retreat. The sea level feedback has greater influence on the ice sheet's stability for the case of the 500 km retreat, rather than the 200 km retreat. The reason is that the former level of retreat involves more ice loss and is achieved over a longer time scale than the latter; therefore, the net sea level fall predicted by the GSCVE sea level model at the grounding line, which acts to compensate for the reversed bed slope, is greater.

3.2. Elastic and Viscous Effects

[24] As we have discussed, the sea level change at a given time in the evolution of the ice sheet is due to both an instantaneous elastic signal associated with ongoing ice and ocean load changes and by a viscous signal that depends on the complete time history of loading changes. Figure 5 explores the relative contribution of these signals to the computed ice sheet evolution for three different values of the initial bed slope ranging from −0.3 to −0.7 m/km. In all cases, ice sheet retreat is initiated through a 60% reduction in the ice-shelf side-drag coefficient. The green line in each frame represents the case where sea level changes are not incorporated into the ice sheet model, and the blue and red lines are the results of simulations that incorporate sea level changes either predicted by the GSCVE sea level model or a special case of this sea level model that only includes an elastically deforming Earth model, respectively. In the first ∼500 years of the simulation (i.e., less than the Earth's Maxwell time), the stabilization associated with the sea level feedback is the same whether the sea level solver adopts an elastic or viscoelastic Earth rheology. On longer timescales, these two cases diverge as the ongoing viscous effects from past ice and ocean load changes become important. The elastic component of sea level change is an important stabilization mechanism throughout the evolution of the ice sheet, and this importance relative to the full viscoelastic case is proportionately greater as the rate of retreat increases or, equivalently, the amplitude of the reversed bed slope increases (Figure 5).

4. Conclusions

[25] Accurate prediction of global sea level requires knowledge of the evolution of marine ice sheets, and it appears that local changes in sea level can have a first order influence upon the rate of mass loss that marine ice sheets undergo and the equilibrium states that they may attain. In a previous paper, we considered the stabilizing influence of sea level changes on the stability of marine ice sheets by coupling the steady state ice sheet model of *Weertman* [1974] to a sea level model that adopted an elastically deforming Earth model [*Gomez et al.*, 2010b]. While the study highlighted the potential importance of the sea level feedback, it was inadequate for the purposes of exploring the influence of this stabilization mechanism on the timescale of ice sheet retreat.

[26] Here, we coupled a gravitationally self-consistent sea level model that incorporates viscoelastic deformation of the Earth [*Kendall et al.*, 2005; *Gomez et al.*, 2010a] to a more realistic, time-evolving marine ice sheet-shelf model [*Pollard and DeConto*, 2007, 2009] and considered the timescale of retreat under a large suite of simulations in which the external forcing, bed slope, and sea level feedback

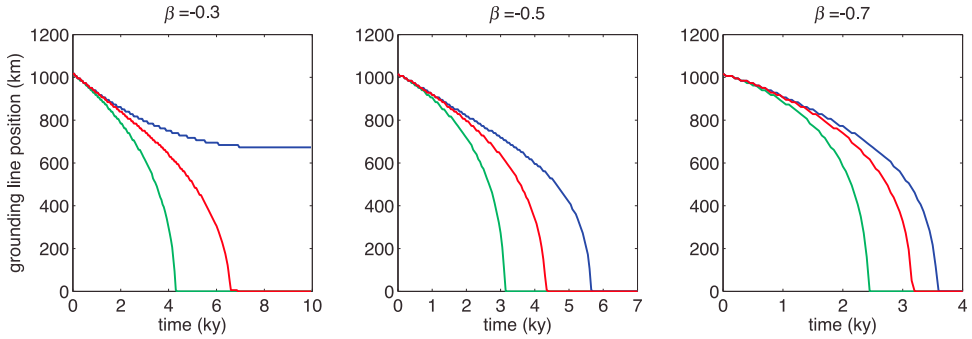

Figure 5. Grounding-line position of the ice sheet model as a function of time, in cases where sea level is not included in the model ice sheet evolution (green); or where the ice sheet model incorporates sea level changes computed using either the full viscoelastic Earth response (blue), or the elastic response alone (red). Results are shown for a range of reversed bed slopes, as labeled on each frame, and in all cases retreat is initiated by a 60% reduction in the side-drag coefficient.

were varied. Our results demonstrate that the sea level fall associated with a retreating ice sheet will slow down and, in the case of shallow reversed bed slopes and/or small external forcing, may even halt the retreat (see Figure 4). Therefore, the stability and motion of the grounding line will depend not only on the local bed slope but also on the magnitude and rate of local sea level change. Changes in local sea level depend upon redistribution of ice mass and both elastic and viscous deformations of the solid Earth, where determining the viscous deformation requires accounting for the full history of ice and ocean loading. In the case of a steady state ice sheet entering into a rapid retreat, viscous effects can be largely neglected for the first several centuries.

[27] We have focused here on ice sheet-wide changes in mass, taking place on millennial timescales. Of course, localized mass loss can occur on shorter timescales. For a given mass loss, the local sea level fall associated with rapid melting will increase as the spatial scale decreases. However, given the existence of an elastic lithosphere, the contribution from viscous effects will generally decrease as the spatial scale of the localized melting is reduced. Thus, the influence of sea level stabilization in the case of century scale and localized melting is worthy of future, detailed study.

[28] Our predictions are based on a 1-D ice sheet model with a simplified bedrock geometry. In future work, we will extend the model to three dimensions and include other factors that influence the evolution of the grounding line, such as lateral stresses, non-uniform bedrock gradients and variable basal conditions. Grounding-line migration in the ice sheet model we have adopted depends on the *Schoof* [2007] flux parameterization, and this should be tested using higher-resolution and higher-order ice sheet models. We also plan to investigate the adequacy of linear or bilinear spatial interpolation in passing fields between the sea level and the ice sheet models (Section 2.3). More generally, it will be important to assess the extent to which the sea level stabilization mechanism discussed herein remains important in the context of more realistic treatments of marine-based outlet glaciers and tidewater glacier environments. We also plan to extend the coupled model to consider the evolution of ice sheets throughout glacial cycles, and in particular since the Last Glacial Maximum. This application may be used, for example, to investigate inter-hemispheric teleconnections between ice sheets [*Denton et al.*, 1986], the timing of ice sheet growth and collapse, and the potential for the sea level mechanism to stabilize the West Antarctic Ice Sheet during interglaciations and terminations.

[29] **Acknowledgments.** The authors thank the reviewers and editors for their helpful comments and suggestions. The authors would also like to acknowledge support from Harvard University (NG, JXM, PH), the Natural Sciences and Engineering Research Council (NG), the U.S. National Science Foundation under grants OCE-1202632, OPP-1043018 and OPP-0424589 (DP) and grant OCE-0960787 (PH), the Canadian Institute for Advanced Research (JXM), and the Paleoclimate Program and the Antarctic Glaciology Program of the NSF (PUC).

References

Dahlen, F. A. (1976), The passive influence of the oceans upon the rotation of the Earth, *Geophys. J. R. Astron. Soc.*, *46*, 363–406, doi:10.1111/j.1365-246X.1976.tb04163.x.

Denton, G. H., T. J. Hughes, and W. Karlén (1986), Global ice-sheet system interlocked by sea level, *Quat. Res.*, *26*, 3–26, doi:10.1016/0033-5894(86)90081-5.

Dupont, T. K., and R. B. Alley (2005), Assessment of the importance of ice-shelf buttressing to ice-sheet flow, *Geophys. Res. Lett.*, *32*, L04503, doi:10.1029/2004GL022024.

Dziewonski, A. M., and D. L. Anderson (1981), Preliminary Reference Earth Model (PREM), *Phys. Earth Planet. Inter.*, *25*, 297–356, doi:10.1016/0031-9201(81)90046-7.

Farrell, W. E., and J. A. Clark (1976), On postglacial sea level, *Geophys. J. R. Astron. Soc.*, *46*, 647–667, doi:10.1111/j.1365-246X.1976.tb01252.x.

Gagliardini, O., G. Durand, T. Zwinger, R. C. A. Hindmarsh, and E. Le Meur (2010), Coupling of ice-shelf melting and buttressing is a key process in ice-sheets dynamics, *Geophys. Res. Lett.*, *37*, L14501, doi:10.1029/2010GL043334.

Goldberg, D., D. M. Holland, and C. Schoof (2009), Grounding line movement and ice shelf buttressing in marine ice sheets, *J. Geophys. Res.*, *114*, F04026, doi:10.1029/2008JF001227.

Gomez, N., J. X. Mitrovica, M. E. Tamisiea, and P. U. Clark (2010a), A new projection of sea level change in response to collapse of marine sectors of the Antarctic Ice Sheet, *Geophys. J. Int.*, *180*, 623–634, doi:10.1111/j.1365-246X.2009.04419.x.

Gomez, N., J. X. Mitrovica, P. Huybers, and P. U. Clark (2010b), Sea level as a stabilizing factor for marine-ice-sheet grounding lines, *Nat. Geosci.*, *3*, 850–853, doi:10.1038/ngeo1012.

Jenkins, A., and C. S. M. Doake (1991), Ice-ocean interaction on Ronne Ice Shelf, Antarctica, *J. Geophys. Res.*, *96*, 791–813, doi:10.1029/90JC01952.

Katz, R. F., and M. G. Worster (2010), Stability of ice-sheet grounding lines, *Proc. R. Soc. A*, *466*, 1597–1620, doi:10.1098/rspa.2009.0434.

Kendall, R. A., J. X. Mitrovica, and G. A. Milne (2005), On post-glacial sea level II. Numerical formulation and comparative results on spherically symmetric models, *Geophys. J. Int.*, *161*, 679–706, doi:10.1111/j.1365-246X.2005.02553.x.

Lambeck, K., C. Smither, and P. Johnston (1998), Sea-level change, glacial rebound and mantle viscosity for northern Europe, *Geophys. J. Int.*, *134*, 102–144, doi:10.1046/j.1365-246x.1998.00541.x.

Lenton, T. M., H. Held, E. Kriegler, J. W. Hall, W. Lucht, S. Rahmstorf, and H. J. Schellnhuber (2008), Inaugural Article: Tipping elements in the Earth's climate system, *Proc. Natl. Acad. Sci. U. S. A.*, *105*, 1786–1793, doi:10.1073/pnas.0705414105.

MacAyeal, D. R., T. A. Scambos, C. L. Hulbe, and M. A. Falhestock (2003), Catastrophic ice-shelf break-up by an ice-shelf-fragment-capsize mechanism, *J. Glaciol.*, *49*(164), 22–36, doi:10.3189/172756503781830863.

Mitrovica, J. X., and A. M. Forte (2004), A new inference of mantle viscosity based upon joint inversion of convection and glacial isostatic adjustment data, *Earth Planet. Sci. Lett.*, *225*, 177–189, doi:10.1016/j.epsl.2004.06.005.

Mitrovica, J. X., M. E. Tamisiea, J. L. Davis, and G. A. Milne (2001), Recent mass balance of polar ice sheets inferred from patterns of global sea-level change, *Nature*, *409*, 1026–1029, doi:10.1038/35059054.

Pollard, D., and R. M. DeConto (2007), A coupled ice-sheet/ice-shelf/sediment model applied to a marine-margin flow line: Forced and unforced variations, in *Glacial Sedimentary Processes and Products*, *Int. Assoc. of Sedimentol. Spec. Publ.*, vol. 39, edited by M. J. Hambrey et al., pp. 37–52, Blackwell, Malden, Mass.

Pollard, D., and R. M. DeConto (2009), Modelling West Antarctic ice sheet growth and collapse through the past five million years, *Nature*, *458*, 329–332, doi:10.1038/nature07809.

Rignot, E. (2006), Changes in ice dynamics and mass balance of the Antarctic ice sheet, *Philos. Trans. R. Soc. A*, *364*, 1637–1655, doi:10.1098/rsta.2006.1793.

Rignot, E., and S. S. Jacobs (2002), Rapid bottom melting widespread near Antarctic Ice Sheet grounding lines, *Science*, *296*, 2020–2023, doi:10.1126/science.1070942.

Scambos, T. A., J. A. Bohlander, C. A. Shuman, and P. Skvarca (2004), Glacier acceleration and thinning after ice shelf collapse in the Larsen B embayment, Antarctica, *Geophys. Res. Lett.*, *31*, L18402, doi:10.1029/2004GL020670.

Schoof, C. (2007), Ice sheet grounding line dynamics: Steady states, stability and hysteresis, *J. Geophys. Res.*, *112*, F03S28, doi:10.1029/2006JF000664.

Shepherd, A., D. J. Wingham, J. A. D. Mansley, and H. F. J. Corr (2001), Inland thinning of Pine Island Glacier, West Antarctica, *Science*, *291*, 862–864, doi:10.1126/science.291.5505.862.

Smith, J. B., et al. (2009), Assessing dangerous climate change through an update of the Intergovernmental Panel on Climate Change (IPCC) "reasons for concern," *Proc. Natl. Acad. Sci. U. S. A.*, *106*, 4133–4137, doi:10.1073/pnas.0812355106.

Thomas, R. H., and C. R. Bentley (1978), A model for Holocene retreat of the West Antarctic Ice Sheet, *Quat. Res.*, *10*, 150–170, doi:10.1016/0033-5894(78)90098-4.

Thomas, R., et al. (2004), Accelerated sea-level rise from West Antarctica, *Science*, *306*, 255–258, doi:10.1126/science.1099650.

Weertman, J. (1974), Stability of the junction of an ice sheet and an ice shelf, *J. Glaciol.*, *13*, 3–11.

Wilchinsky, A. V. (2009), Linear stability analysis of an ice sheet interacting with the ocean, *J. Glaciol.*, *55*, 13–20, doi:10.3189/002214309788608895.

Wingham, D. J., D. W. Wallis, and A. Shepherd (2009), Spatial and temporal evolution of Pine Island Glacier thinning, 1995–2006, *Geophys. Res. Lett.*, *36*, L17501, doi:10.1029/2009GL039126.

P. U. Clark, Department of Geosciences, Oregon State University, Corvallis, OR 97331, USA.

N. Gomez, P. Huybers, and J. X. Mitrovica, Department of Earth and Planetary Sciences, Harvard University, 20 Oxford St., Cambridge, MA 02138, USA. (ngomez@fas.harvard.edu)

D. Pollard, Earth and Environmental Systems Institute, 2217 Earth-Engineering Sciences Bldg., Pennsylvania State University, University Park, PA 16802, USA.